

Build them up and break them down

Tight junctions of cell lines expressing typical hepatocyte polarity with a varied repertoire of claudins

Brigitte Grosse,^{1,2} Jeril Degrouard,² Danielle Jaillard² and Doris Cassio^{1,2,*}

¹Inserm, UMR-S 757; Orsay, France; ²Université Paris-Sud; Orsay, France

Keywords: tight junctions, hepatocyte polarity, bile canaliculi, WIF-B9, 11-3, Can 3-1, Can 10, claudins, paracellular permeability, calcium depletion

Abbreviations: TJ, tight junction; MDCK, Madin-Darby Canine Kidney; BC, bile canaliculi; DPPIV, dipeptidyl peptidase IV; PFIC1, progressive familial intrahepatic cholestasis type 1; BRIC1, benign recurrent intrahepatic cholestasis type 1; PFIC2, progressive familial intrahepatic cholestasis type 2; NISCH, Neonatal ichthyosis and sclerosing cholangitis; TEM, transmission electron microscopy; GJ, gap junction; MV, microvilli; GAPDH, Glyceraldehyde 3-phosphate dehydrogenase; RT-PCR, reverse transcription-polymerase chain reaction; PM, plasma membrane; C5-DBM-SM, N-[5-(5,7-dimethyl BODIPY)-l-pentanoyl]-Derythro-sphingosyl phosphocholine; TER, transepithelial resistance; AMP, AMP-activated protein kinase; LKB1, Liver kinase B1; AJ, adherent junction; DF-BSA, defatted bovine serum albumin

Tight junctions (TJs) of cells expressing simple epithelial polarity have been extensively studied, but less is known about TJs of cells expressing complex polarity. In this paper we analyzed, TJs of four different lines, that form bile canaliculi (BC) and express typical hepatocyte polarity; WIF-B9, 11-3, Can 3-1, Can 10. Striking differences were observed in claudin expression. None of the cell lines produced claudin-1. WIF-B9 and 11-3 expressed only claudin-2 while Can 3-1 and Can 10 expressed claudin-2,-3,-4,-5. TJs of these two classes of lines differed in their ultra-structure, paracellular permeability, and robustness. Lines expressing a large claudin repertoire, especially Can 10, had complex and efficient TJs, that were maintained when cells were depleted in calcium. Inversely, TJs of WIF-B9 and 11-3 were leaky, permissive and dismantled by calcium depletion. Interestingly, we found that during the polarization process, TJ proteins expressed by all lines were sequentially settled in a specific order: first occludin, ZO-1 and cingulin, then JAM-A and ZO-2, finally claudin-2. Claudins expressed only in Can lines were also sequentially settled: claudin-3 was the first settled. Inhibition of claudin-3 expression delayed BC formation in Can 10 and induced the expression of simple epithelial polarity. These results highlight the role of claudins in the settlement and the efficiency of TJs in lines expressing typical hepatocyte polarity. Can 10 seems to be the most promising of these lines because of its claudin repertoire near that of hepatocytes and its capacity to form extended tubular BC sealed by efficient TJs.

Introduction

Tight junctions (TJs) are essential structures of polarized cells.¹ They form an apical/basolateral intra-membrane diffusion barrier in the outer leaflet of the plasma membrane (fence function), and control the extent and selectivity of diffusion along the paracellular pathway (gate function). Defects in TJ components, contribute to inherited diseases¹⁻⁴ and several TJ proteins are targeted by viruses, bacteria and other pathogens.^{1,2,4,5} Consequently TJ have an important role in the pathogenesis of a wide range of diseases.²⁻⁴

TJs have been extensively studied in tissues or cell lines expressing simple epithelial polarity, such as Madin-Darby kidney cells (MDCK). However, although the first constitutive proteins of

TJs were isolated from liver,^{6,7} studies of TJs in liver, and in particular in hepatocytes, are not numerous. Hepatocytes are the principal cells of liver. They express complex polarity, with several apical and basolateral poles per cell.⁸ The union of the apical poles of adjacent and front-facing hepatocytes forms a thin and complex tridimensional network of tubular bile canaliculi, which is delimited by TJs, and into which bile is secreted. The volume of the canalicular network in a human liver is estimated at 3.5 cm³ and the length of the TJs sealing this network at 20,000 km.⁹

Hepatocyte polarity is difficult to maintain in vitro and only a few hepatic polarized cell lines have been developed.¹⁰ From the unpolarized Fao rat hepatoma line, we isolated, by hybridization¹¹⁻¹³ or transient growth in spheroids,¹⁴ several cell lines expressing typical hepatocyte polarity. These lines are

*Correspondence to: Doris Cassio; Email: doris.cassio@u-psud.fr

Submitted: 04/06/13; Revised: 05/28/13; Accepted: 05/29/13

Citation: Grosse B, Degrouard J, Jaillard D, Cassio D. Build them up and break them down: Tight junctions of cell lines expressing typical hepatocyte polarity with a varied repertoire of claudins. Tissue Barriers 2013; 1:e25210; <http://dx.doi.org/10.4161/tisb.25210>

characterized by the formation of bile canaliculi (BC) (Fig. 1A), in the membrane of which canalicular proteins, such as dipeptidyl peptidase IV (DPPIV), are localized (Fig. 1B).

Several of these hepatic polarized lines are currently used as models to study hepatocyte features¹⁵⁻¹⁹ or liver diseases, e.g., Wilson's disease,²⁰⁻²² PFIC1 (progressive familial intrahepatic cholestasis type 1),²³ BRIC1 (benign recurrent intrahepatic cholestasis type 1),²³ PFIC2 (progressive familial intrahepatic cholestasis type 2)²⁴ and NISCH (neonatal ichthyosis and sclerosing cholangitis) syndrome.²⁵ In earlier work we analyzed the localization of a few tight junctional constituents, such as occludin and ZO-1, in these cell lines.^{14,26,27} In more recent work, the role of JAM-A²⁸ and claudin-2²⁹ in the WIF-B line and its subclone WIF-B9 as well as the role of claudin-1 in Can 10 subclones²⁵ were examined. However, complete analysis of TJs of polarized hepatic cell lines has not yet been performed. In the present work we studied in a panel of four cell lines expressing typical hepatocyte polarity, WIF-B9, 11-3, Can 3-1, Can 10, the structure and the efficiency of TJs, the settlement of ten TJ proteins throughout the polarization process, and the impact of TJ perturbing treatments.

Results

TJs were first studied in fully polarized cultures once a high percent of cells formed BC (85, 70, 80 and 95%, respectively for WIF-B9, 11-3, Can 3-1 and Can 10 cells). Then, TJs were examined throughout the polarization process. Finally, the impact of TJ perturbing treatments was analyzed.

The bile canaliculi of the polarized cell lines are sealed by developed tight junctions. Polarized cultures were examined by transmission electron microscopy (TEM). A minimum of 30 BC were examined per cell line. All examined BC were lined by microvilli and sealed by TJs (Fig. 2). For WIF-B9 and 11-3 cells, BC were simple and formed by the union of two to three cells (Fig. 2). The majority of BC formed by Can 3-1 cells were simple (Fig. 2), although a few extended BC were observed. By contrast, the majority of BC of Can 10 cells were complex and extended, and several cells were implicated in the formation of each extended BC. An example of an extended Can 10 BC with numerous visible TJs is shown in Figure 2. The general aspect of TJs was similar in all cell lines, although TJs of Can 3-1 seemed thicker and those of Can 10 longer (Fig. 2).

TJs were also examined by freeze fracture. The TJs of WIF-B9, 11-3 and Can 3-1 cells, were composed of only a few rows of fibrils. The TJs of Can 10 were complex and composed of numerous fibrils organized in an extended and highly reticulated network (Fig. 3), evocative of the network of mature TJs in rat liver.^{9,30}

The polarized cell lines do not express the same repertoire of claudins. The expression levels of ten TJ proteins were determined (Fig. 4A). Similar levels of JAM-A, occludin, ZO-1, ZO-2, cingulin were produced by all cell lines. By contrast, striking differences were observed for claudins. Like Fao cells, WIF-B9 and 11-3 produced only claudin-2. Can 3-1 and Can 10 produced, in addition to claudin-2, claudin-3,-4,-5; this claudin

repertoire was near to that of hepatocytes, which produced claudin-1,-2,-3,-5³¹ (Fig. 4A). None of the cell lines produced claudin-1. The non-expression of claudin-1 and the mRNA expression pattern of claudin-3 by the different cell lines were confirmed by reverse transcription-polymerase chain reaction (RT-PCR) (Fig. 4B).

WIF-B9 cells are segregated rat x human hybrid cells, selected for the retention of the human chromosome X, which carries the claudin-2 gene.³² It was thus possible that WIF-B9 cells produce rat and human claudin-2. Since the antibody used for detecting claudin-2 was not species-specific, we used RT-PCR. We found that WIF-B9 cells contained claudin-2 transcripts of both species (Fig. 4B).

The proteins of tight junctions are appropriately localized in polarized hepatic lines. The localization of TJ proteins was analyzed by immunofluorescence. The results obtained were summarized in Figure 4C and some examples were shown in Figure 4D. In the non polarized parental cells Fao, TJ proteins were either present in the cytoplasm, or unevenly distributed at the plasma membrane (PM), as illustrated for claudin-2 and cingulin, respectively (Fig. 4D). In polarized lines, all TJ proteins, (except claudin-4 in Can 3-1), were localized as belts sealing simple or extended BC (Fig. 4D). This localization was similar to that previously reported for claudin-1 and occludin in polarized primary human hepatocyte cultured on collagen,³³ and for occludin in polarized primary rat hepatocytes cultured in collagen sandwich.³⁴

The tight junctions of the hepatic polarized cells are functional and differ in their paracellular permeability. We then analyzed the efficiency of TJs. The capacity to form a diffusion barrier to lipids in the PM, the fence function, was first examined (Fig. 5). Cells were incubated at 4°C with a fluorescent analog of sphingomyelin, C5-DMB-SM/DF-BSA, washed and examined immediately. In all cells the basolateral PM domain was fluorescent, whereas most BC were unlabeled (Fig. 5A). A low fraction of fully or partially labeled BC was observed for WIF-B9, 11-3 (Fig. 5B), and Can 3-1, suggesting defective tightness of a number of TJs in those lines. By contrast 95% of BC of Can 10 were unlabeled, (Fig. 5A), including the longer and more complex BC (Fig. 5C), attesting to the efficacy of TJs and their competence as an intra-membrane diffusion barrier.

The second TJ function examined was the selectivity of diffusion along the paracellular pathway, the gate function. This was performed by TEM using lanthanum hydroxide and tannic acid (Fig. 6A) and by evaluating the accessibility of BC to fluorescent dextrans of various molecular weights (Fig. 6B). Lanthanum hydroxide and tannic acid accumulated under TJs and did not pass into the BC of the four cell lines (Fig. 6A b, d-f and h, j-l), except in a minority of WIF-B9 and 11-3 cells, respectively (Fig. 6A a, g and c, i). Significant differences in dextran paracellular diffusion were found. The percent of BC accessible to dextrans was similar for WIF-B9 and 11-3, and decreased significantly for Can 3-1 and Can 10, this decrease being more important for Can 10. These differences were observed for each dextran. These results demonstrate that TJs of WIF-B9 and 11-3 are the most permissive, those of Can 10 the most selective.

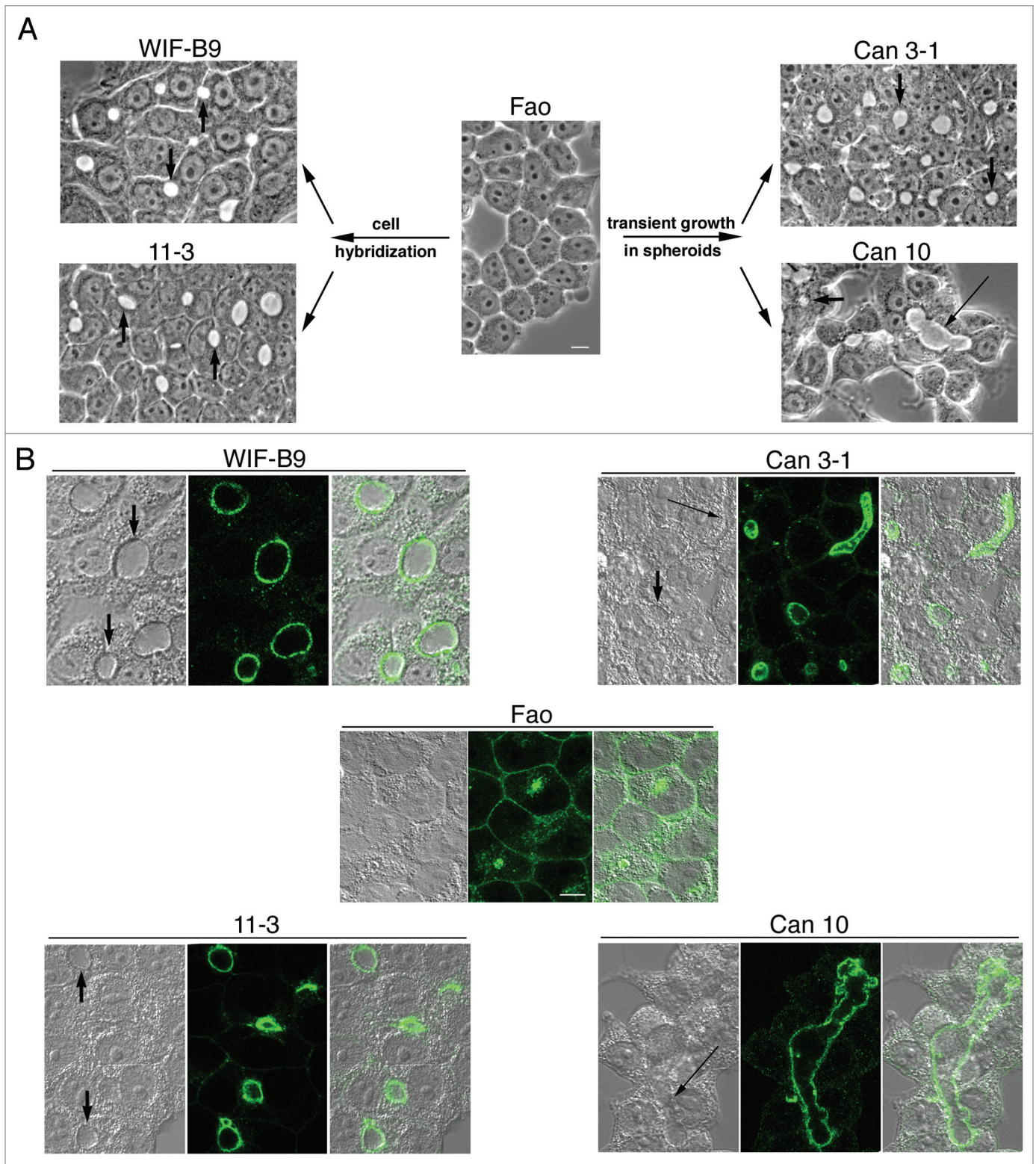


Figure 1. Cell lines expressing the typical hepatocyte polarity. **(A)** Generation of these lines (for details see refs, 7–10) and phase contrast images of living cells (shown at the same magnification). Numerous bile canaliculi (phase lucent structures) are present in cultures of all lines, except in the non-polarized parental Fao line. Some canaliculi are indicated by arrows. Note that Can 10 cells form extended canaliculi (long arrow). Bar, 10 μ m. **(B)** Immunolocalization of the canalicular protein DPPIV analyzed by confocal microscopy. For each cell line an xy section taken in the middle of the cell layer is presented (middle) with the corresponding interferential contrast image (left) and the composite image (right). DPPIV is present at the plasma membrane and intracellularly in the non-polarized parental Fao line, while it is localized at the membrane of bile canaliculi of each of the four polarized lines. Some canaliculi are indicated by arrows on the interferential contrast images. Can 10 (and to a lesser extent Can 3-1) form long and extended bile canaliculi (long arrows). Confocal images are shown at the same magnification. Bar, 10 μ m.

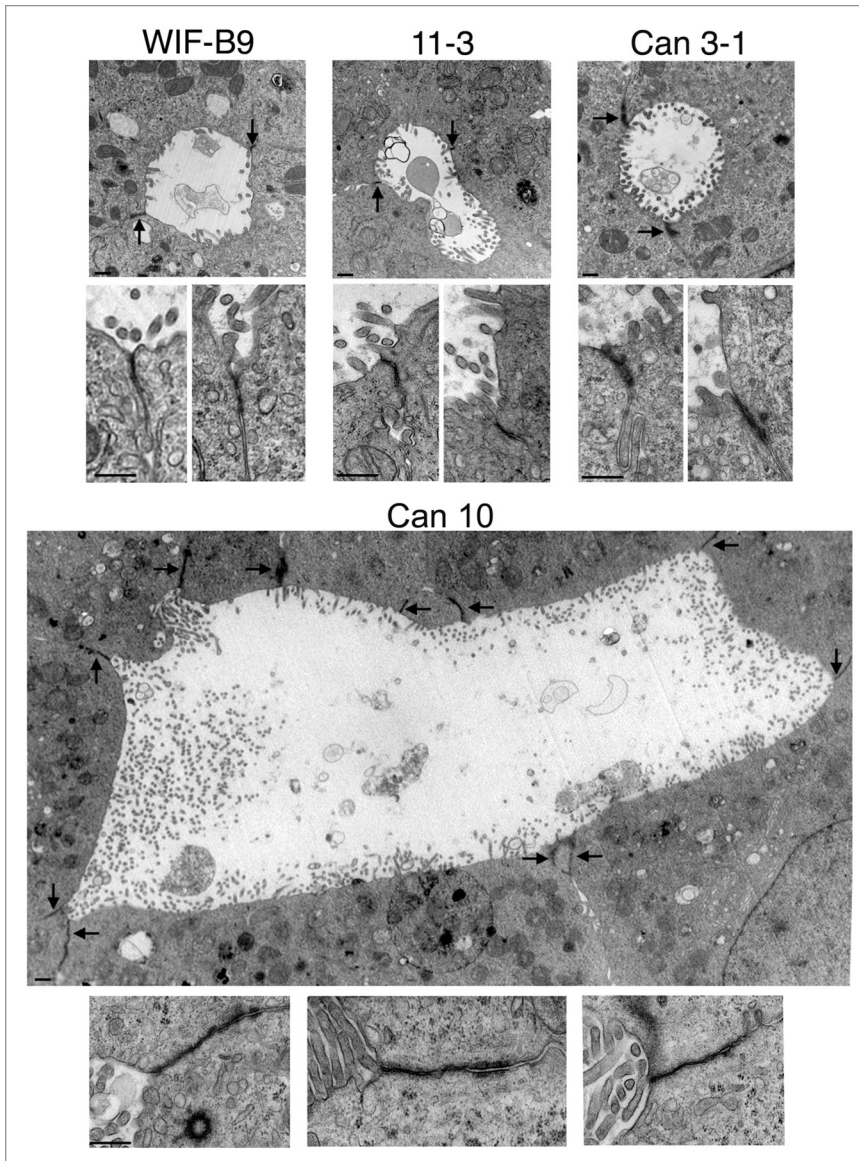


Figure 2. Transmission electron microscopy pictures of bile canaliculi and tight junctions of cell lines expressing typical hepatocyte polarity. For each cell line, a representative bile canaliculus (upper part) and two or three examples of tight junctions (lower part) are presented. The images of bile canaliculi are shown at the same magnification, with sealing tight junctions indicated by arrows. The images of tight junctions are presented at a 3-fold higher magnification than canaliculi. Note the high number of cells and junctions implicated in the formation of the canaliculus of Can 10. Bars, 500 nm.

The proteins of tight junctions are sequentially settled throughout the polarization process. TJs are complex scaffoldings. Little is known about their assembly and maturation. To address this question the settlement of proteins of TJs was followed throughout the polarization of the different cell lines. We previously showed that the formation of BC in WIF-B9 and 11-3 cells is a slow process, which requires, even at high plating density, several days to be complete, and which is preceded by the transient expression of the simple epithelial polarity.^{14,26,27} The polarization process of Can 3-1 and Can 10 is different. BC were

formed rapidly after plating and cells expressing simple epithelial polarity were rarely observed.¹⁴

The localization of TJ proteins was examined in cells forming BC, from 8 h to 10 d after plating (Fig. 7A). The accessibility of BC to fluorescent dextrans of various molecular weights was measured in parallel (Fig. 7B). Surprisingly, we observed that TJ proteins were sequentially settled in TJs sealing BC, according to a similar order in all cell lines. Among the constitutive TJ proteins, claudin-3 (only expressed in Can clones) and occludin were early settled, followed by JAM-A and other claudins. Claudin-2 was by far the last to be settled and in Can 3-1 and Can 10 cells, this protein was settled only in a fraction of TJs even after 10 d (Fig. 7A). The early settlement of claudin-3 and the delayed settlement of claudin-2 in TJs of Can 10 cells are illustrated in Figure 7C. Among the TJ-associated proteins ZO-1 and cingulin were early settled, whereas ZO-2 was completely settled only after 4–6 d (Fig. 7A). Except claudin-2, all TJ proteins were fully settled 4 d after plating. The paracellular permeability to dextrans decreased progressively in all lines during the sequential settlement of TJ proteins, and stabilized after several days when most TJ proteins were settled (Fig. 7B).

Is the sequence of TJ protein settlement characteristic of polarized clones expressing typical hepatocyte polarity? To answer this question we examined renal MDCK cells that express simple epithelial polarity. Transepithelial resistance (TER) was used to follow the establishment of MDCK polarity and the settlement of TJ proteins was analyzed throughout the polarization process (Fig. 8). We observed that TJ proteins were sequentially settled according to an order similar to that found in Can lines: occludin and claudin-3 were settled first; claudin-2 was the last and its complete settlement occurring only after 5 d (Fig. 8A). TER increased and stabilized when all TJ proteins were settled (Fig. 8B).

The settlement of TJ proteins was also analyzed (data not shown), in three Can 10 clones expressing claudin-1.²⁵ In these clones, the expression of claudin-1 did not change the sequential settlement of the other claudins, claudin-3 was still the first to be settled, claudin-2 the last, and claudin-1 settled in between, as shown in MDCK cells (Fig. 8B).

Polarity and TJs of cell lines expressing a large repertoire of claudins are maintained during calcium depletion. Calcium depletion has been widely used to perturb adherent junctions (AJs) and TJs of polarized cells expressing simple epithelial

polarity, such as MDCK,³⁵ T84,³⁶ and mouse mammary epithelial cells.³⁷ The impact of calcium depletion was examined by analyzing the presence of BC and the localization of TJ proteins in calcium-depleted cells (Fig. 9A, B). The percent of WIF-B9 and 11-3 cells forming BC progressively decreased during calcium depletion (Fig. 9A) and canalicular proteins, such as HA4, were redistributed in the cytoplasm (Fig. 9C). By contrast, BC were maintained in calcium-depleted Can 3-1 and Can 10 cells (Fig. 9A), and canalicular proteins, such as HA4, were maintained at the membrane of BC, even after a 6 h-calcium depletion (Fig. 9C). The whole TJ proteins (Fig. 9B) were discontinuously redistributed all over the PM in WIF-B9 and 11-3, whereas they were maintained as continuous belts sealing BC in Can 3-1 and Can 10, as illustrated for ZO-1 (Fig. 9C). Thus, calcium depletion disrupts apical polarity and TJs of WIF-B9 and 11-3 cells, but not those of Can 3-1 and Can 10 cells. The TJ gate function of Can lines was followed during calcium depletion and after calcium replenishment (Fig. 9D). This function was ineffectual in the absence of calcium in Can-3-1 cells, whereas relative functionality was maintained in Can 10 cells. TJs of both lines regained their initial efficacy after calcium replenishment.

The silencing of claudin-3 delays bile canaliculi formation of Can 10 cells and induces the expression of simple epithelial polarity. Finally, we perturbed TJ settlement. We choose the line with the most complex and robust TJs, namely Can 10, and we decided to silence claudin-3, because this protein is early settled (Fig. 7). Three siRNA were used. All were efficient and inhibited claudin-3 expression at the transcriptional and the translational level (Fig. 10A and B), the siRNA2 being the most efficient. This effect was maximal after 48 h of treatment. The expression of other TJ proteins was not or slightly affected, as shown for ZO-1 (Fig. 10B). Compared with control cells and cells transfected with scrambled siRNA, cells in which claudin-3 was silenced formed fewer BC (Fig. 10C). Surprisingly, most cells expressed simple epithelial polarity, as attested by the localization examined by confocal microscopy of TJ proteins, such as ZO-1, claudin-5 and occludin (Fig. 10D). Consequently, the transient reduction of claudin-3 expression perturbs the polarization process of Can 10 but does not prevent the formation of TJs.

Unfortunately, the TJ gate function of Can 10 cells silenced for claudin-3 could not be analyzed; Can 10 cells did not grow at confluency and therefore it was impossible to obtain appropriate cell layers for TER and flux measurements. However the fence function was examined and was efficient, since apical proteins, such as DPP IV, were present at the apex of silenced cells (Fig. S1).

Discussion

In this work, we analyzed TJs of several cell lines expressing typical hepatocyte polarity¹²⁻¹⁴ to obtain information on their structure, composition, efficiency, stability and settlement, and to compare the results with simple epithelial cells.

TJ structure, TJ efficiency, and claudin expression. The hepatic polarized lines can be grouped in two classes. The first class comprises WIF-B9 and 11-3. These lines form only simple

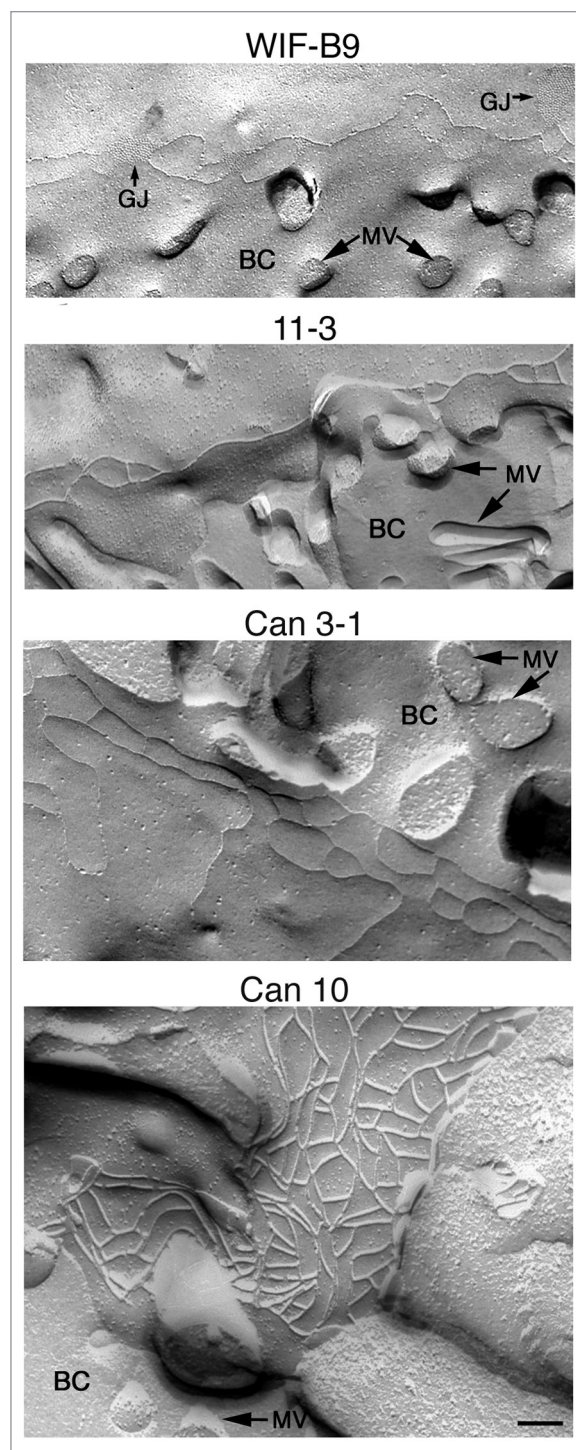


Figure 3. Freeze-fracture replicas of cell lines expressing typical hepatocyte polarity. BC, bile canaliculus; GJ, gap junction; MV, microvilli. Bar, 100 nm.

BC. Their TJs are formed by few rows of fibrils. They are relatively leaky, and their paracellular permeability to dextrans is high. The second class comprises Can 3-1 and Can 10. These lines are able to form BC between several cells. Their TJs, in particular those of Can 10, are formed by a complex network of numerous fibrils. They are more selective and their paracellular

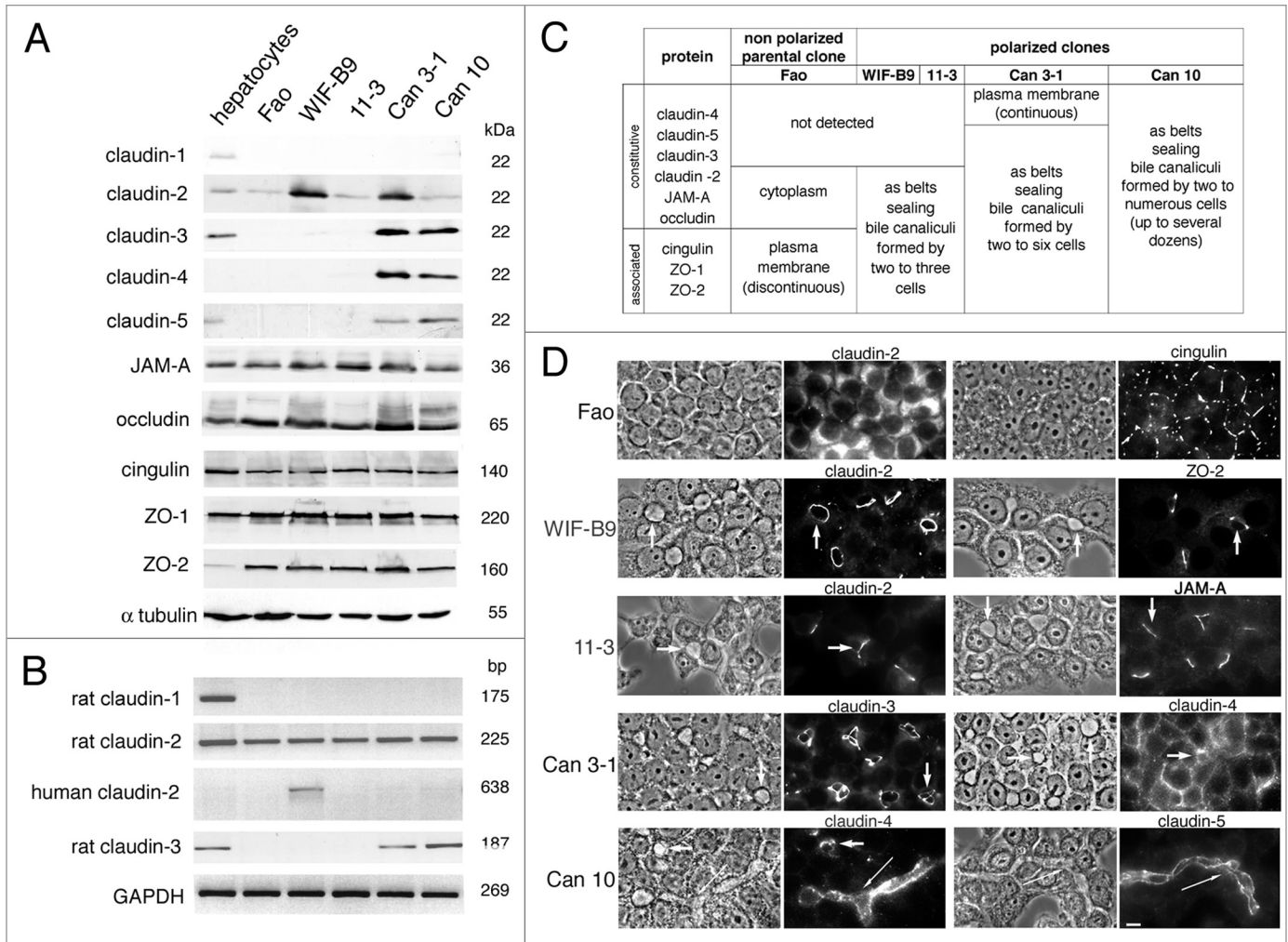


Figure 4. Expression and localization of tight junction (TJ) proteins in cell lines expressing typical hepatocyte polarity. Fully polarized cultures were examined. **(A)** Western blot. Each lane was loaded with a cell lysate aliquot containing 25 μ g total protein. **(B)** RT-PCR. For western blot and RT-PCR, experiments were performed three times with lysates or RNA preparations from two to three independent cultures; one representative experiment is shown. **(C)** Summary of the localization of ten TJ proteins. Experiments were performed at least three times on three independent cultures. **(D)** Images of the localization of some TJ proteins; for each case, the corresponding phase-contrast image is given on the left. Some bile canaliculi (BC) are indicated by arrows (short arrows for BC formed between two cells, long arrows for extended BC). Bar, 10 μ m.

permeability is low. Briefly, TJs of the second class are more complex and more efficient.

This better efficiency is most probably linked to their claudin repertoire. Like their unpolarized Fao parental line, WIF-B9 and 11-3 express only claudin-2, this claudin being typical of leaky TJs.^{38,39} In contrast Can 3-1 and Can 10 express claudin-2,-3,-4,-5, a repertoire near that of hepatocytes.³¹ In fully polarized cultures of all clones, each claudin (except claudin-4 in Can 3-1) is localized with the other TJ proteins, in TJs sealing BC. Thus, the TJs of the two classes of clones are not built with the same composition of claudins.

The underlying reason for the activation of the expression of claudin-3,-4,-5 in Can lines remains to be clarified. We previously determined that E-cadherin, which is known to play a crucial role in establishing polarity⁴⁰ is overproduced in Can clones.¹⁴ We are currently studying if proteins implicated in cell polarity and TJ formation, such as other claudins,¹ crumbs,⁴¹ AMP-activated

protein kinase (AMPK),³⁴ or liver kinase B1 (LKB1),³⁴ are activated or overexpressed in these lines.

Settlement of TJ proteins. Surprisingly, we found that the settlement of TJ proteins throughout the cell polarization process was a sequential process occurring in a specific order; this order was similar for the four hepatic cell lines and MDCK cells. This result suggests that TJ construction patterns are similar regardless of the type of polarity expressed. This hypothesis demands to be tested in other polarized cell lines. TJ protein localization and settlement should be analyzed when hepatocyte polarity is maintained (isolated hepatocyte couplets),⁴² restored (collagen sandwich culture of primary hepatocytes) or built de novo (liver regeneration). Little information exists on TJ protein settlement in these particular cases: occludin is correctly localized as soon as BC are formed in collagen sandwich cultures;³⁴ claudin-3 and ZO-1 are present in newly formed TJs after one day of partial hepatectomy, whereas occludin is almost absent.⁴³

Our studies strongly suggest that the integration of TJ proteins in TJs does not occur randomly, but instead follows a specific temporal pattern that very likely reflects the sequential steps of TJ assembly. According to this hypothesis, the TJ proteins that settle first, might constitute the core of the TJ scaffolding and the other TJ proteins, particularly claudin-2, that are integrated later, would be more peripheral.

TJ functionality throughout the settlement of TJ proteins. TJ functionality was examined during the settlement of TJ proteins. BC visible by phase contrast microscopy were formed as early as 8 h after plating. At that point, only a small fraction of WIF-B9 and 11-3 cells was implicated in the formation of BC, whereas almost all cells of Can lines formed BC. Nevertheless, in all lines and as previously shown for WIF-B9,²⁷ apical proteins were exclusively localized at the PM of all new formed canaliculi, whereas basolateral proteins were excluded from these structures. Thus, the fence function is fully functional at an early stage, long before the settlement of TJ proteins is completed. This is very likely related to the early settlement of proteins, such as occludin and ZO-1.

By contrast, the maximal efficiency of the gate function was attained later, when all TJ proteins, in particular claudins (except claudin-2 for Can clones), were settled. This result is in good agreement with the role attributed to claudins in the gate function.^{1,44,45} It also supports previous experiments showing that the gate function can be uncoupled from the fence function.⁴⁶⁻⁴⁸

TJ and calcium depletion. Calcium depletion induced a rapid disappearance of BC and the delocalization of TJ proteins in clones of the first class. By contrast, BC and TJs were maintained during calcium depletion in Can lines, although the cohesion between neighboring cells was reduced (Fig. 9) showing that calcium deprivation had a real effect on the cell layer organization. This difference cannot be attributed to a higher expression of E-cadherin in Can clones, since we previously showed that WIF-B9, 11-3, Can 3-1 and Can 10 cells produce similar amounts of E-cadherin (respectively, 4.5, 5.5, 4.7, and 4.9 times the level of Fao cells).^{14,49}

These results indicate that TJs of polarized cells expressing hepatocyte polarity are less sensitive to calcium depletion when they are composed of several claudins and that they can be maintained, even when the adhesion between cells is weakened. These findings are in good agreement with studies showing that the TJ organization of hepatocytes is not altered in calcium deprivation-induced cholestasis⁵⁰ and is maintained in calcium-depleted collagen sandwich cultures of primary hepatocytes, treated by AMK1 and LKB1 activators.³⁴ It should be noted that although the fence function of TJs is maintained in Can cells during calcium depletion, the gate function is less efficient in Can 10 and completely lost in Can 3-1 cells. Consequently, expression and correct localization of TJ proteins in cells, do not guarantee TJ functionality, in particular for the gate function.

TJs constituted of several claudins in cells expressing hepatocyte polarity, such as Can 10 cells or Par1b-MDCK,⁵¹ appear to be less sensitive to calcium depletion than comparable TJs in MDCK cells expressing simple epithelial polarity. This difference could be due to a stronger association of TJs with components of the bile canalicular skeleton, particularly actin,^{52,53} in cells expressing hepatocyte polarity.

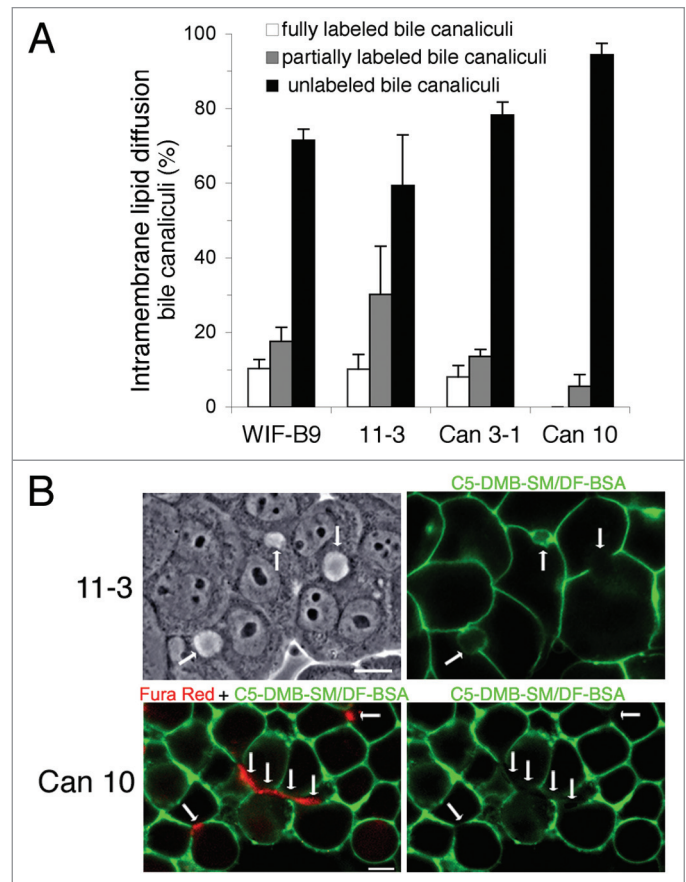


Figure 5. TJ Fence function of cell lines expressing typical hepatocyte polarity. Fully polarized cultures were incubated with the fluorescent lipid C5-DBM-SM/DF-BSA, at 2°C for 30 min. The PM basolateral domain of all cells was intensely fluorescent, while most bile canaliculi were unlabeled. (A) Quantification of unlabeled, partially- and fully-labeled bile canaliculi. Values are means from three independent cell cultures of each cell line. (B) 11-3 cells: one field with three bile canaliculi (arrows), one unlabeled (right), one partially-labeled (left) and one fully-labeled (middle), is shown with the corresponding phase-contrast image on the left. (C) Can 10 cells. Confocal microscopy images of a field containing several bile canaliculi (arrows), including a long canaliculus (marked by four vertical arrows) are shown. Here, the cells were first incubated with Fura Red, AM to better visualize the bile canaliculi. Note that the bile canaliculi into which Fura Red was transported (image on the left) were unlabeled with the fluorescent lipid (image on the right). Bars, 10 μ m.

Silencing of TJ proteins and changes in polarity. The role of TJ proteins was studied, using the overexpression strategy in polarized cells,⁵⁴⁻⁵⁷ or TJ-free cells.^{58,59} It was also evaluated by generating knockout mice⁶⁰ and by analyzing polarized cell lines deficient in one specific TJ protein. Several TJ proteins were silenced by RNA interference in MDCK cells. The consequences on the polarity state of MDCK cells depended on the protein silenced.⁶¹⁻⁶³ No change in polarity was observed in cells silenced for claudin-1,-2,-3,-4,-7, respectively.⁶¹ Silencing of ZO-1 causes a delay in TJ formation.⁶² Silencing of ZO-2 leads to an atypical monolayer architecture.⁶³

Few TJ proteins were silenced in cells expressing the typical hepatocyte polarity. In all cases the polarity was affected. BC

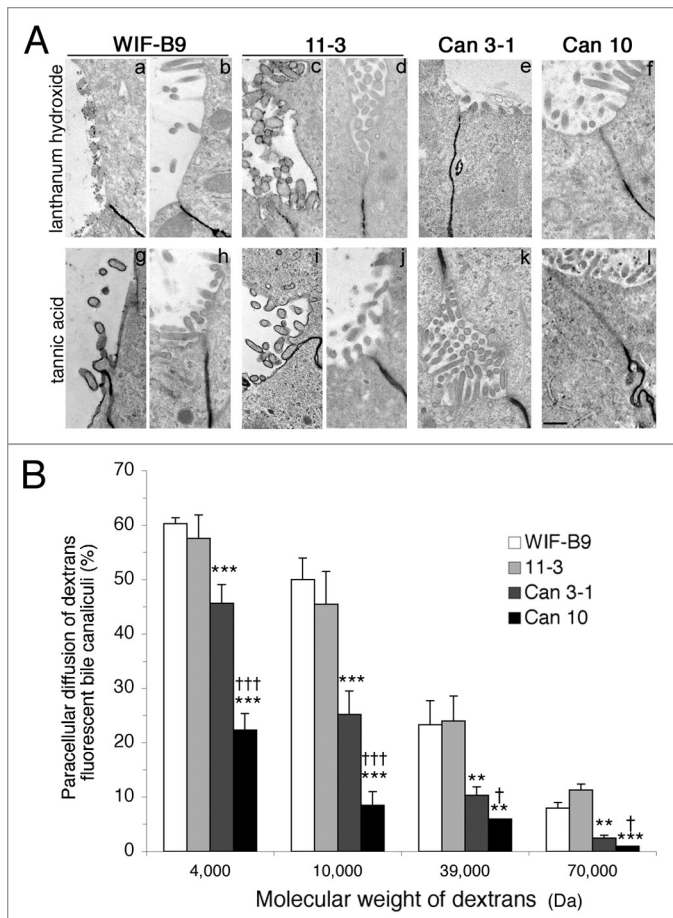


Figure 6. TJ gate function of cell lines expressing typical hepatocyte polarity. **(A)** Transmission electron microscopy pictures. In Can 3-1 (e,k) and Can 10 cells (f,l), lanthanum hydroxide and tannic acid accumulated under tight junctions (TJs) without penetration into bile canaliculi, demonstrating the intactness of TJs in these lines. In WIF-B9 and 11-3 cells, deposition of lanthanum and tannic acid was observed in a minority of bile canaliculi (a, g and c, i), but the majority was unlabeled (b, h, and d, l). Bar, 500 nm. **(B)** Paracellular diffusion into bile canaliculi of FITC-dextrans of different molecular weights. Values are means of three independent cultures of each cell line, ** $p < 0.01$, *** $p < 0.001$ as compared with WIF-B9, and 11-3 cells; * $p < 0.05$, *** $p < 0.001$ as compared with Can 3-1 cells.

formation was reduced in WIF-B9 cells silenced for JAM-A²⁸ and claudin-2²⁹ and in Can 10 cells silenced for claudin-3 (Fig. 10). Moreover, Can 10 cells deprived in claudin-3 expressed the simple epithelial polarity. The factors implicated in this switch in polarity of Can 10 cells remain to be determined. It should be noted that this switch occurred in cells going to polarize (claudin-3 siRNA being transfected at the time of cell plating) and was not observed for cells already polarized and forming BC (data not shown). Thus, claudin-3 expression would be required for the establishment of hepatocyte polarity but not for its maintenance. Similarly, it has been shown that E-cadherin expression is necessary for the establishment of epithelial polarity in MDCK cells, while it is dispensable for maintaining this polarity.⁶⁴ In future studies it will be essential to discriminate the role of TJ proteins during TJ assembly from their role on TJ maintenance.

MDCK express the simple epithelial polarity. However over-expression of Par1b/EMK1/MARK2 in these cells induces the expression of hepatocyte polarity and a hepatocyte mode of apical protein trafficking.^{65,66} Hepatocyte-like polarity in MDCK was also observed following expression of dominant negative RhoA and constitutively active Rac1.^{8,67} These examples and the one of Can 10 cells silenced for claudin-3 demonstrate the flexibility of the polarized phenotype and illustrate the fact that it is possible to intervene in the branching decision between simple epithelial and hepatocyte polarity.⁵¹

Usefulness of the two classes of cell lines. WIF-B9 and 11-3 lines have TJs containing only claudin-2. They will very useful for testing the role of other claudins, by introducing non-expressed claudins either one by one, or in combination. They are also appropriate to study the transition between simple epithelial polarity and hepatocyte polarity.^{14,26} Finally, since WIF-B9 cells form functional connexin 32-constituted gap junctions (GJs),⁶⁸ they represent an adapted model to study the interactions between TJs and GJs, in particular the association of connexins with several TJ proteins.⁶⁹

Can 3-1 and Can 10 cells have TJs composed of a large repertoire of claudins. Thus, they are rather suited for a strategy of silencing of TJ proteins, as reported here for claudin-3 in Can10 cells. Furthermore the density-dependent polarized phenotype of Can 3-1,¹⁴ deserves to be further analyzed. Cell density is also a pivotal parameter during cultivation of primary hepatocytes.⁷⁰ Can 10 line is the most promising line, because of its claudin repertoire, its efficient TJs and its capacity to form extended tubular BC.^{14,18,21} Moreover, it is easy to transfect.²⁵ Can 10 represents an attractive model to identify, in dividing cells, the mechanisms by which AMPK and its upstream kinase, LKB1, regulate tubular canalicular network formation and maintenance.^{34,71} On a more general level, Can 10 is appropriate for analyzing the formation, expansion and branching of lumens.^{72,73}

The different hepatic polarized lines could also be useful for deciphering how the cytoskeleton, in particular the actin-cytoskeleton, regulates AJs and TJs integrity and remodeling.⁷⁴ However, even if in vitro models are useful, they have limitations that is important to be aware. Therefore the results obtained with these models should be as much as possible confronted to the in vivo situations.

Materials and Methods

Materials. Coon's modified F-12 medium (F6636), the antibiotic, antimycotic solution (A5955), the mounting medium (M1289), TriReagent (T9424) and antibodies against α tubulin (T-9026) were obtained from Sigma. Calcium-free Coon's modified F12 medium was from Eurobio (Les Ulis, France). HAT supplement (21060) L-glutamine (25030-04), fetal bovine serum (10270-106, batch 41F5392K), and trypsin-EDTA (25300-054) were obtained from Gibco BRL. Glutaraldehyde (16200) and osmium tetroxide (19150) were from Electron Microscopy Sciences. Lanthanum nitrate (R1207), cacodylate (R1103) and epon were obtained from Agar Scientific. Tannic acid (1746) was from A.R. Mallinckrodt Inc. Antibodies directed against claudin-1, -2, -3, -4, -5 (51-9000,

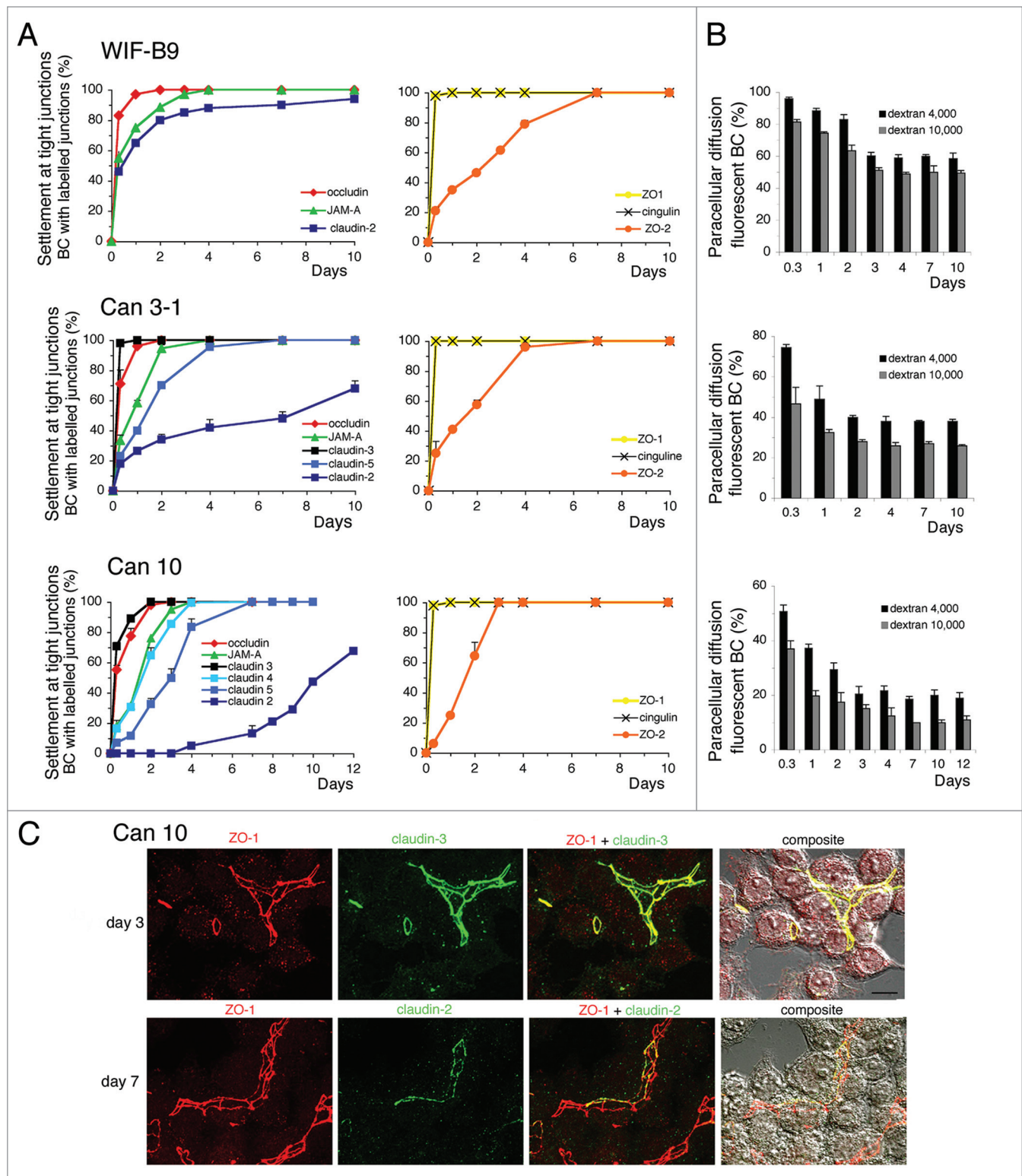


Figure 7. Settlement of tight junction (TJ) proteins and paracellular permeability throughout the polarization of cell lines expressing typical hepatocyte polarity. **(A)** Settlement of constitutive (left) and associated- (right) TJ proteins at TJs sealing bile canalicular (BC), analyzed by immunolocalization. **(B)** Paracellular permeability throughout the settlement process. Values are means of three independent cultures of each cell line; 11-3 values (not shown) were similar to those shown here for WIF-B9 cells. In Can3-1 cells, claudin-4 was not settled at TJs as the other TJ proteins, and was present at the whole plasma from the first day. **(C)** Localization of claudin-3 with ZO-1 on day 3, and of claudin-2 with ZO-1 on day 7, by confocal microscopy in Can 10 cells. The localization of the TJ proteins (compilation of 21–24 xy sections) is shown, followed by the merge image and the composite image (interferential contrast image + merge image). Note that on day 3 claudin-3 and ZO-1 were completely settled at the TJs sealing bile canalicular, whether bile canalicular were formed between two cells or more. By contrast, claudin-2 was not completely settled on day 7. It was either absent or partially present at the TJs where ZO-1 localized. Bar 10 μ m.

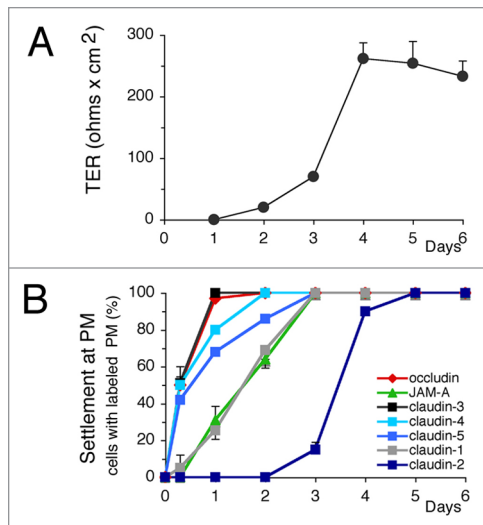


Figure 8. Transepithelial resistance measurement (TER) and settlement of tight junction (TJ) proteins throughout the polarization of MDCK cells. **(A)** TER. **(B)** Settlement of TJ proteins at the plasma membrane. Values are means of three independent cultures. ZO-1 and cingulin (not shown) were settled very early, as shown for hepatic cell lines (Fig. 7A).

51–100, 34–1700, 32–9400, 34–1600), JAM-A (36–1700), occludin (33–1500) were from Zymed. Mouse antibodies directed against ZO-2 (611560) were from BD-Transduction Laboratories. Rabbit polyclonal antibodies directed against cingulin were generously provided by S. Citti (Universita' di Padova).⁷⁵ Rat monoclonal antibodies against ZO-1 were obtained from B. Stevenson.⁷⁶ Antibodies against the apical proteins dipeptidyl peptidase IV (DPP-IV) and HA4 were kindly given by A. Hubbard (Johns Hopkins University).^{12,13} Horseradish peroxidase-linked secondary antibodies were obtained from GE Healthcare (NA934, NA931, NA932). Fluorescent Alexa 568 (A-11031, A-11036, A-11077) and 488 (A-11001, A-11034) secondary antibodies, the fluorescent lipid, N-[5-(5,7-dimethyl BODIPY)-l-pentanoyl]-Derythro-sphingosyl phosphocholine (C5-DMB-SM) (D3522) and Fura Red™, AM (F-3031) were from Molecular Probes. FITC-conjugated dextrans were obtained from Sigma (FD4, FD40S) and Molecular Probes (D1821, D1823). Lipofectamine™ RNAiMAX (13-78-075), SuperScript II Reverse Transcriptase (were obtained from Invitrogen).

Hepatocytes, cell lines and general culture conditions. Isolated rat hepatocytes were prepared as previously described.⁷⁷ The polarized cell lines, WIF-B9, 11-3, Can 3-1 and Can 10, were derived from Fao, a sub-clone of the unpolarized rat hepatoma H4IIEC3 line.^{13,14} Madin-Darby canine kidney (MDCK) cells were obtained from ATCC (CCL-34™). Cell culture was performed in Coon's modified F-12 medium, in Petri dishes (Falcon) or on glass coverslips (CML), exactly as described.¹¹ MDCK cells were also cultured in inserts (Falcon, 0.4 μm pore size, 353090). For WIF-B9 and 11-3 cells, medium was supplemented with HAT (10⁻⁴ M hypoxanthine, 4 × 10⁻⁷ M aminopterin, 1.6 × 10⁻⁵ M thymidine). Fao, WIF-B9, 11-3, Can 10 and MDCK cells, were plated at 4 × 10³/cm². Can 3-1 cells were plated at 10⁵/cm²; this high density is necessary for Can 3-1 polarization (Peng et

al. 2006). Cells grown in dishes were used for EM analysis, RNA extraction or protein lysate preparation. Cells on coverslips were used for immunolocalization, or for fluorescent lipid and FITC-dextrans diffusion studies. Cells in inserts were used for measurement of TER. All cultures tested negative for *Mycoplasma* using the Mycoalert test (Lonza, LT07–318).

Electron microscopy. Cells were fixed with 2% glutaraldehyde or 2% glutaraldehyde/1% lanthanum nitrate in 0.1 M sodium cacodylate buffer, pH 7.3, for 1 h at room temperature, and postfixed with 1% OsO₄ in the same buffer for 1 h at room temperature. Some of the samples fixed with 2% glutaraldehyde were after postfixation, incubated with 1% tannic acid in 0.1 M sodium cacodylate buffer, pH 7.3 for 1 h at room temperature.⁷⁸ All samples were dehydrated through a graded ethanol series, and embedded in Epon 812. Ultrathin sections (70 nm) obtained with an ultra microtome (Ultracut UCT Leica), were double stained with uranyl acetate and lead citrate and then examined with a Philips EM208 electron microscope operating at 80 kV.

For freeze-fracture, cells fixed in 2.5% glutaraldehyde for 1 h at room temperature, were cryoprotected with 30% glycerol in 0.1 M phosphate buffer for 30 min at 4°C and frozen in ethane. Samples were fractured in a freeze-fracture device (Cryofract, Balzers BAF 400T) under vacuum at -150°C and shadowed with platinum-carbon. Replicas, were examined after cleaning, using the electron microscope indicated above.

Western blotting. Cells were lysed exactly as previously described.⁷⁹ Proteins (25 μg) from lysate aliquots were electrophoretically separated using SDS-PAGE and transferred to nitrocellulose (GE Healthcare, Hybond ECL, RPN 203D). Immunoblotting was performed with antibodies specific to claudin-1 (1/200), claudin-2 (1/200), claudin-3 (1/200), claudin-4 (1/400), claudin-5 (1/200), JAM-A (1/100), occludin (1/200), cingulin (1/5000), ZO-1 (undiluted), ZO-2 (1/250), α tubulin (1/5000). Appropriate peroxidase-conjugated secondary antibodies were used and peroxidase activity was detected by enhanced chemiluminescence (GE Healthcare, RPN2105). ImageJ software was used for densitometric analysis.

RNA isolation and reverse-transcription-PCR (RT-PCR). Total RNA was isolated using Tri Reagent and 1 μg of total RNA was converted to first-strand cDNA using superscript™ II reverse transcriptase enzyme according to the manufacturer's instructions. Primers and PCR conditions are summarized in Table 1.

Immunolocalization. Cells plated on glass coverslips were rinsed three times in phosphate-buffered saline (PBS), fixed for 30 min at 4°C in ethanol, followed by 1 min at room temperature in acetone. After fixation, indirect immunofluorescence was performed,⁷⁷ using primary antibodies specific to claudin-1 (1/100), claudin-2 (1/100), claudin-3 (1/100), claudin-4 (1/200), claudin-5 (1/100), JAM-A (1/100), occludin (1/200), cingulin (1/1500), ZO-1 (undiluted), ZO-2 (1/200), and appropriate Alexa Fluor-conjugated secondary antibodies (1/500). Cells were analyzed with a Zeiss Axioskop fluorescence microscope. Images were collected through a X40 oil-immersion objective with a CCD camera (Orca, Hamamatsu) and digitized with the HCI imaging software (Hamamatsu). Alternatively cells were examined with a Zeiss LSM 510 confocal microscope, with a X63 objective. Series

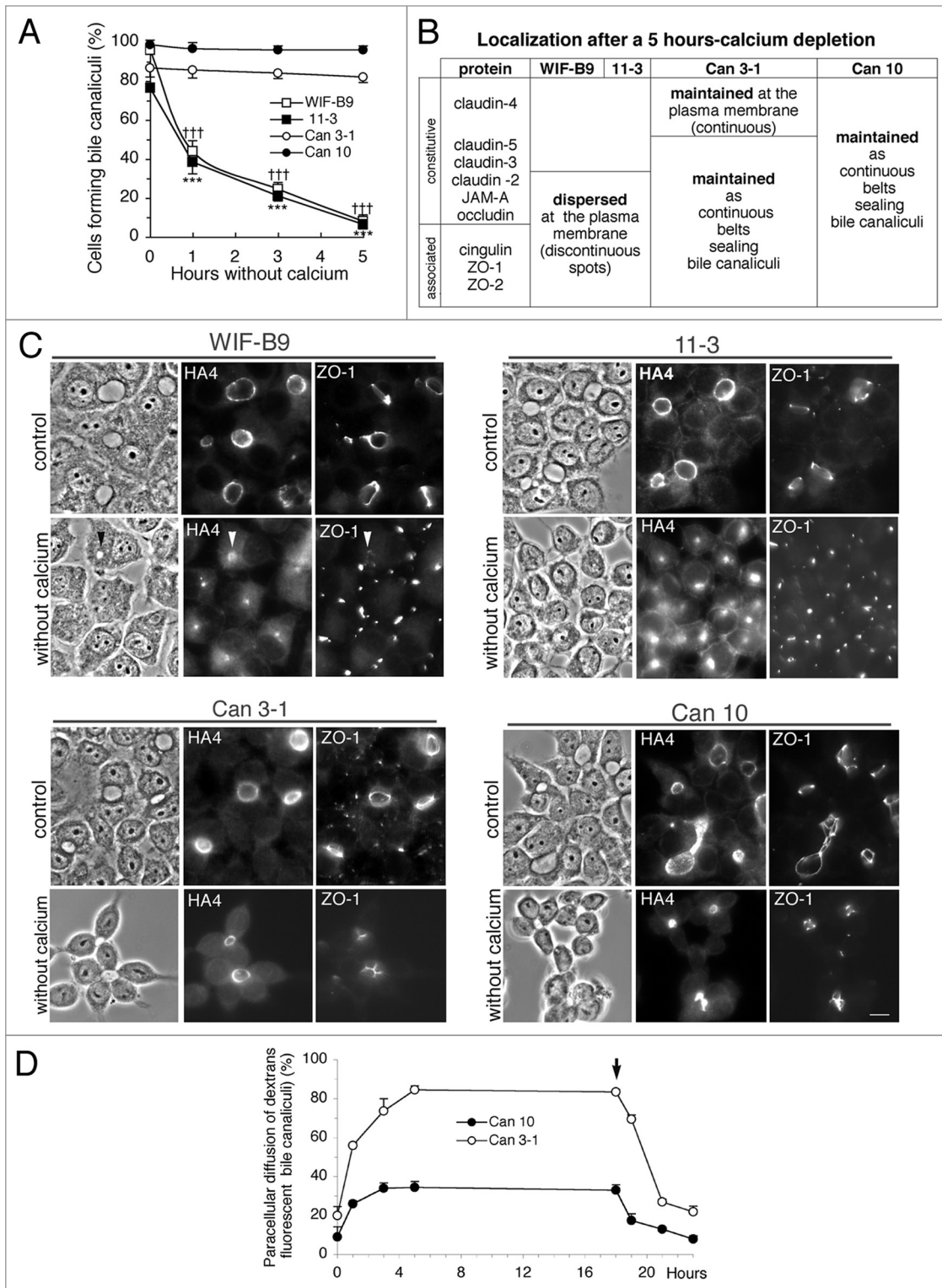


Figure 9. Impact of calcium depletion on polarized cultures of cell lines expressing typical hepatocyte polarity. **(A)** Impact of calcium deprivation on bile canaliculi. Values are means of three independent cultures of each cell line. *** $p < 0.001$ for WIF-B9 cells as compared with Can 10 and Can 3-1 cells; ††† $p < 0.001$ for 11-3 cells as compared with Can 10 and Can 3-1 cells. **(B)** Summary of the localization of tight junction proteins after a 5 h-calcium depletion. **(C)** Immunolocalization of the canalicular protein HA4 and the tight junction-associated protein ZO-1 in cells cultured with calcium (control) and in calcium cells depleted of calcium for 5 h. Note the disappearance of bile canaliculi and the change of localization of HA4 and ZO-1 in WIF-B9 and 11-3 cells depleted of calcium. In both cases, ZO-1 is dispersed at the plasma membrane, whereas HA4 is present in an intracellular compartment, often visible in phase contrast in WIF-B9 (arrowheads). Such changes do not occur in Can 3-1 and Can 10 cells depleted of calcium. **(D)** Evolution of the paracellular diffusion of 39,000 Da FITC-dextran in bile canaliculi of Can 3-1 and Can 10 cells depleted of calcium for a period of 18 h and then renewed with calcium containing medium. The arrow indicates when the cells were replenished with calcium.

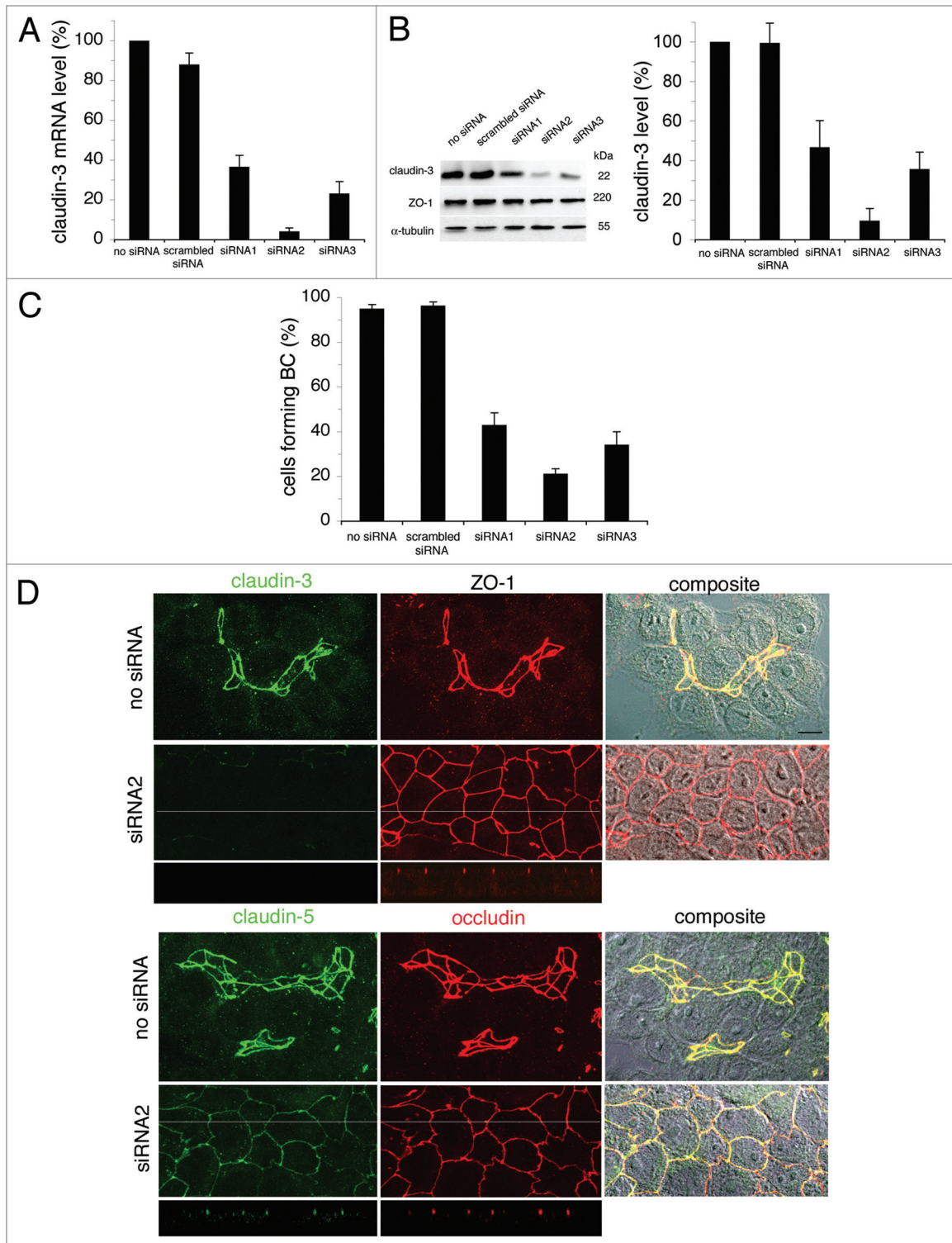


Figure 10. Impact of silencing claudin-3 on Can 10 polarity. Cells transfected either by Lipofectamine with no siRNA, scrambled siRNA or three different claudin-3 siRNA were examined 48 h after transfection. **(A)** RT-qPCR of one representative experiment. Claudin-3 mRNA level is expressed as the percentage of the level of cells treated with no siRNA. **(B)** Western blot. An immunoblot corresponding to the experiment shown in A is presented on the left. Densitometric analysis of immunoblots obtained from three independent experiments is on the right. Claudin-3 level, normalized with α -tubulin as internal control, was expressed as the percentage of claudin-3 level of cells treated with no siRNA. **(C)** Analysis of cells forming bile canaliculi. Values are means of three independent experiments. **(D)** Co-localization of claudin-3 with ZO-1, and claudin-5 with occludin, studied by confocal microscopy. In each case, the localization of each tight junction protein (compilation of 20–27 xy sections) is shown, followed by a composite image (interferential contrast image with the merge image) (right). For cells treated with claudin-3 siRNA2, xz sections taken as indicated (thin white lines) on the corresponding xy compilations are also presented. Bar, 10 μ m.

Table 1. Sequences of primers and conditions used for RT-PCR

Gene	Primer sequence (forward)	Primer sequence (reverse)	Amplicon size (bp)	Number of cycles	Annealing Temperature (0°C)
rat GAPDH	5'-TCC CTC AAG ATT GTC AGC AA-3'	5'-AGA TCC ACA ACG GAT ACA TT-3'	269	25	55°C
rat claudin-1	5'-CAG GAG CCT CGC CCC GCA G-3'	5'-GAA GCG CAA CCC CGC AG-3'	175	30	58°C
rat claudin-2	5'-GGC ACA TCG ATT GCC ATG CTG-3'	5'-GGC CAG CGA GGA CAT TGC AC-3'	225	30	58°C
human claudin-2	5'-TGG CCT CTC TTG CCT CCA ACT TGT-3'	5'-TTG ACC AGG CCT TGG AGA GCT C-3'	638	35	55°C
rat claudin-3	5'-GCC GTT AGC GTG CTC CGT CC-3'	5'-GAC GTG CCG GTG ATC TCC AGG-3'	187	30	55°C

of xy sections were taken in 0.3 μm steps. Images were processed using Photoshop 7 software (Adobe).

Intramembrane diffusion of fluorescent lipids. Complexes of the fluorescent analog of sphingomyelin, C₅-DMB-SM, with defatted bovine serum albumin (DF-BSA) were prepared as described.⁸⁰ Cells grown on coverslips were washed with HSFM buffer (10 mM Hepes, 145 mM sodium chloride, 1 mM sodium pyruvate, 10 mM glucose, 3 mM calcium chloride, pH 7.2) at 2°C, incubated with 5 μM of C₅-DMB-SM/DF-BSA for 30 min at 2°C, washed with HSFM and observed under epifluorescence illumination within 5–10 min after mounting. BC were first identified under phase contrast illumination, and then categorized according to labeling (fully, or partially, or unlabeled). Three coverslips were examined from each culture (four fields per coverslip and at least 200 observed BC). To better identify the BC of Can 10, cells were first incubated 30 min at 37°C with 3 μM Fura Red in serum-free medium without phenol red.

Paracellular diffusion of FITC-labeled dextrans. The paracellular diffusion of FITC-dextrans (molecular weights: 4,000, 10,000, 39,000, 70,000 Da) into the BC was performed as previously described.¹² Cells grown on glass coverslips were washed once with serum-free medium, incubated with 3 mg/ml FITC-dextrans for 10 min at 37°C, then washed twice with cold serum-free medium and observed within 5–10 min after mounting. Fluorescent BC were counted and expressed as a percentage of the total number of BC observed by phase contrast. Three coverslips were examined from each culture (four fields per coverslip and at least 200 observed BC).

Settlement of tight junction proteins. WIF-B9, 11-3 and Can 10 cells were plated on glass coverslips at $4 \times 10^3/\text{cm}^2$; Can 3-1 cells at $10^5/\text{cm}^2$. The localization of TJ proteins was examined by immunofluorescence in cells forming BC, from 8 h to 10 d after plating. BC sealed with labeled TJ proteins were counted and expressed as a percentage of the total number of BC observed by phase contrast. Three coverslips were examined from each culture and at least 200 BC were examined by coverslip. The paracellular diffusion of FITC-dextrans (molecular weights 4,000 and 10,000 Da) into the BC was studied in parallel, as described above.

MDCK cells were plated on glass coverslips and in inserts at $4 \times 10^3/\text{cm}^2$. The transepithelial resistance (TER) and the localization of TJ proteins were examined from 8 h to 6 d after plating. Cells with TJ proteins-labeled PM were counted and expressed as a percentage of the total number of cells observed by phase contrast. Three coverslips were examined at each time and at least 200 cells were examined per coverslip.

Transepithelial resistance measurement. Transepithelial resistance (TER) was measured with a Millicel apparatus (Millipore). All TER values were obtained using at least three inserts (6–8 measurements per insert at each time) after background subtraction (i.e., filter and culture medium).

Calcium depletion. Cells were plated on glass coverslips and cultured for at least 7 d until they reached maximum density and polarity. They were rinsed three times, switched in calcium-free medium without serum ($[\text{Ca}^{2+}] \leq 25 \mu\text{M}$), and examined at regular intervals. Control cells were maintained in calcium-containing medium without serum. Cells forming BC were counted (on phase contrast micrographs for WIF-B9, 11-3 and Can 3-1 cells and after immunolocalization of HA4 for Can 10 cells). At least 300 cells and six different cell fields were examined at each time. In parallel, TJ proteins were immunolocalized. Cells of Can 3-1 and Can 10 were maintained in calcium-free medium for 18 h and then renewed with calcium (1.12 mM) containing medium. The paracellular diffusion into the BC of both lines of 39,000 Da FITC-dextran was studied as described above, throughout the calcium switch experiment.

Silencing of claudin-3. siRNA1 (5'-GCU CUC AUC GUG GUG UCU A-3'), siRNA2 (5'-CCA ACU GCG UAC AAG AUG A-3'), and siRNA3 (5'-CCC ACC AAG AUC CUC UAU U-3') duplexes targeted to rat claudin-3, were chemically synthesized by Eurogentec. Scrambled siRNA (SR-CL000-05) was obtained from the same purchaser. Can 10 cells were plated at $2.5 \times 10^4/\text{cm}^2$ in medium without antibiotics and immediately transfected using Lipofectamine™ RNAiMAX (Invitrogen) in optiMEM medium (Invitrogen), according to the manufacturer's instructions. Final concentrations were 40 nM for siRNA and 2 $\mu\text{L}/\text{mL}$ for Lipofectamine™ RNAiMAX. Cells were examined two to three days after siRNA transfection. Claudin-3 expression (RT-qPCR, western blotting) and the polarity state of Can 10 cells were analyzed. Cells forming BC were counted on phase contrast micrographs after immunolocalization of HA4. The localization of claudin-3, claudin-5, occludin, and ZO-1 was performed by immunofluorescence and analyzed by confocal microscopy.

RT-qPCR. The extraction of total RNA and the reverse transcription were performed as described above. Real time qPCR was performed using Chromo 4 system (Bio-Rad). Reaction mixture was composed by 1x SYBR Green Master Mix, 3 pmol of each primer and cDNA (1/20th RT reaction). Primers for rat Claudin-3 were 5'-GTG GCC ATC GCA GCT ACT-3' and 5'-CCT GTC TCT GCC CAC TAT GAG-3'. Rat GAPDH and rat βActin were used as internal controls. Primers were 5'-TCC CTC AAG ATT GTC AGC AA-3' and 5'-AGA TCC ACA ACG

GAT ACA TT-3', and 5'-ATC GTG GGC CGC CCT AGG CAC-3' and 5'-TGG CCT TAG GGT TCA GAG GGG C-3', respectively. Quantification was performed by software Opticon monitor3 (Bio-Rad).

Statistical analysis. Data were expressed as means \pm standard deviation. Statistical analyses were performed using Student t-test, with a p value < 0.05 being considered statistically significant.

Disclosure of Potential Conflicts of Interest

The authors declare that there are no conflicts of interest.

Acknowledgments

We greatly thank Pedro Rodriguez, Jean-Pierre Lechaire and Ghislaine Frebourg for the preparation of the freeze fractures replica. We are grateful to Ann Hubbard, Sandra Citti and

Bruce R. Stevenson, for kindly providing antibodies. We thank Severine Boufflers for her participation to immunolocalization experiments, Valérie Nicolas (IFR141, Plateforme Imagerie, Université de Pharmacie, Chatenay Malabry, France) and Isabelle Garcin for help with confocal analysis. We are grateful to Pascal Colosetti for careful reading of the manuscript. Finally, we warmly thank Nadya Yousef for examination of the manuscript, linguistic corrections and useful comments and Emmanuel Gonzales for his interest in this work and helpful discussions.

Supplemental Materials

Supplemental materials may be downloaded here: www.landesbioscience.com/journals/tissuebarriers/2013TISSBARRIERO33R-Sup.pdf

References

- Balda MS, Matter K. Tight junctions at a glance. *J Cell Sci* 2008; 121:3677-82; PMID:18987354; <http://dx.doi.org/10.1242/jcs.023887>.
- Cerejido M, Contreras RG, Flores-Benitez D, Flores-Maldonado C, Larre I, Ruiz A, et al. New diseases derived or associated with the tight junction. *Arch Med Res* 2007; 38:465-78; PMID:17560451; <http://dx.doi.org/10.1016/j.armed.2007.02.003>.
- Lai-Cheong JE, Arita K, McGrath JA. Genetic diseases of junctions. *J Invest Dermatol* 2007; 127:2713-25; PMID:18007692; <http://dx.doi.org/10.1038/sj.jid.5700727>.
- Sawada N. Tight junction-related human diseases. *Pathol Int* 2013; 63:1-12; PMID:23356220; <http://dx.doi.org/10.1111/pin.12021>.
- Benedicto I, Molina-Jiménez F, García-Buey L, Gondar V, López-Cabrera M, Moreno-Otero R, et al. Role of tight junctions in hepatitis C virus infection. *Rev Esp Enferm Dig* 2012; 104:255-63; PMID:22662778; <http://dx.doi.org/10.4321/S1130-01082012000500006>.
- Furuse M, Hirase T, Itoh M, Nagafuchi A, Yonemura S, Tsukita S, et al. Occludin: a novel integral membrane protein localizing at tight junctions. *J Cell Biol* 1993; 123:1777-88; PMID:8276896; <http://dx.doi.org/10.1083/jcb.123.6.1777>.
- Furuse M, Fujita K, Hiiiragi T, Fujimoto K, Tsukita S. Claudin-1 and -2: novel integral membrane proteins localizing at tight junctions with no sequence similarity to occludin. *J Cell Biol* 1998; 141:1539-50; PMID:9647647; <http://dx.doi.org/10.1083/jcb.141.7.1539>.
- Braiterman L, Hubbard A. Hepatocyte surface polarity: its dynamic maintenance and establishment. In Arias IM, ed. *The liver biology and pathobiology*. Fifth edition. Wiley-Blackwell publication. 2009:73-106.
- Landmann L, Stieger B. Tight junctions in liver disease. In Cerejido M, Anderson J, eds. *Tight junctions*. Second edition. Boca Raton. CRC Press 2001:575-97.
- Decaens C, Durand M, Grosse B, Cassio D. Which in vitro models could be best used to study hepatocyte polarity? *Biol Cell* 2008; 100:387-98; PMID:18549352; <http://dx.doi.org/10.1042/BC20070127>.
- Cassio D, Hamon-Benais C, Guérin M, Lecoq O. Hybrid cell lines constitute a potential reservoir of polarized cells: isolation and study of highly differentiated hepatoma-derived hybrid cells able to form functional bile canaliculi in vitro. *J Cell Biol* 1991; 115:1397-408; PMID:1955480; <http://dx.doi.org/10.1083/jcb.115.5.1397>.
- Ihrke G, Neufeld EB, Meads T, Shanks MR, Cassio D, Laurent M, et al. WIF-B cells: an in vitro model for studies of hepatocyte polarity. *J Cell Biol* 1993; 123:1761-75; PMID:7506266; <http://dx.doi.org/10.1083/jcb.123.6.1761>.
- Shanks MR, Cassio D, Lecoq O, Hubbard AL. An improved polarized rat hepatoma hybrid cell line. Generation and comparison with its hepatoma relatives and hepatocytes in vivo. *J Cell Sci* 1994; 107:813-25; PMID:8056838.
- Peng X, Grosse B, Le Tiec B, Nicolas V, Delagebeaudeuf C, Bedda T, et al. How to induce non-polarized cells of hepatic origin to express typical hepatocyte polarity: generation of new highly polarized cell models with developed and functional bile canaliculi. *Cell Tissue Res* 2006; 323:233-43; PMID:16231191; <http://dx.doi.org/10.1007/s00441-005-0067-2>.
- Majewski JL, Yang VW. The class I alcohol dehydrogenase gene is glucocorticoid-responsive in the rat hepatoma microcell hybrid cell line, 11-3. *Alcohol Clin Exp Res* 1995; 19:1430-4; PMID:8749806; <http://dx.doi.org/10.1111/j.1530-0277.1995.tb01003.x>.
- Schaffert CS, Toderlo SL, McVicker BL, Tuma PL, Sorrell MF, Tuma DJ. WIF-B cells as a model for alcohol-induced hepatocyte injury. *Biochem Pharmacol* 2004; 67:2167-74; PMID:15135311; <http://dx.doi.org/10.1016/j.bcp.2004.01.022>.
- Wakabayashi Y, Dutt P, Lippincott-Schwartz J, Arias IM. Rab11a and myosin Vb are required for bile canaliculi formation in WIF-B9 cells. *Proc Natl Acad Sci U S A* 2005; 102:15087-92; PMID:16214890; <http://dx.doi.org/10.1073/pnas.0503702102>.
- Cassio D, Macias RI, Grosse B, Marin JJ, Monte MJ. Expression, localization, and inducibility by bile acids of hepatobiliary transporters in the new polarized rat hepatocyte cell lines, Can 3-1 and Can 10. *Cell Tissue Res* 2007; 330:447-60; PMID:17909858; <http://dx.doi.org/10.1007/s00441-007-0494-3>.
- McVicker BL, Rasineni K, Tuma DJ, McNiven MA, Casey CA. Lipid droplet accumulation and impaired fat efflux in polarized hepatic cells: consequences of ethanol metabolism. *Int J Hepatol* 2012; 2012:978136; PMID:22506128; <http://dx.doi.org/10.1155/2012/978136>.
- Braiterman L, Nyasae L, Guo Y, Bustos R, Lutsenko S, Hubbard A. Apical targeting and Golgi retention signals reside within a 9-amino acid sequence in the copper-ATPase, ATP7B. *Am J Physiol Gastrointest Liver Physiol* 2009; 296:G433-44; PMID:19033537; <http://dx.doi.org/10.1152/ajpgi.90489.2008>.
- Hernandez S, Tsuchiya Y, García-Ruiz JP, Laloti V, Nielsen S, Cassio D, et al. ATP7B copper-regulated traffic and association with the tight junctions: copper excretion into the bile. *Gastroenterology* 2008; 134:1215-23; PMID:18395099; <http://dx.doi.org/10.1053/j.gastro.2008.01.043>.
- Pujol AM, Cuillel M, Jullien AS, Lebrun C, Cassio D, Mintz E, et al. A sulfur tripod glycoconjugate that releases a high-affinity copper chelator in hepatocytes. *Angew Chem Int Ed Engl* 2012; 51:7445-8; PMID:22730309; <http://dx.doi.org/10.1002/anie.201203255>.
- Folmer DE, van der Mark VA, Ho-Mok KS, Oude Elferink RP, Paulusma CC. Differential effects of progressive familial intrahepatic cholestasis type 1 and benign recurrent intrahepatic cholestasis type 1 mutations on canalicular localization of ATP8B1. *Hepatology* 2009; 50:1597-605; PMID:19731236; <http://dx.doi.org/10.1002/hep.23158>.
- Gonzales E, Grosse B, Cassio D, Davit-Spraul A, Fabre M, Jacquemin E. Successful mutation-specific chaperone therapy with 4-phenylbutyrate in a child with progressive familial intrahepatic cholestasis type 2. *J Hepatol* 2012; 57:695-8; PMID:22609309; <http://dx.doi.org/10.1016/j.jhep.2012.04.017>.
- Grosse B, Cassio D, Yousef N, Bernardo C, Jacquemin E, Gonzales E. Claudin-1 involved in neonatal ichthyosis sclerosing cholangitis syndrome regulates hepatic paracellular permeability. *Hepatology* 2012; 55:1249-59; PMID:22030598; <http://dx.doi.org/10.1002/hep.24761>.
- Decaens C, Rodriguez P, Bouchaud C, Cassio D. Establishment of hepatic cell polarity in the rat hepatoma-human fibroblast hybrid WIF-B9. A biphasic phenomenon going from a simple epithelial polarized phenotype to an hepatic polarized one. *J Cell Sci* 1996; 109:1623-35; PMID:8799849.
- Decaens C, Cassio D. Spatiotemporal expression of catenins, ZO-1, and occludin during early polarization of hepatic WIF-B9 cells. *Am J Physiol Cell Physiol* 2001; 280:C527-39; PMID:11171572.
- Braiterman LT, Heffernan S, Nyasae L, Johns D, See AP, Yutzy R, et al. JAM-A is both essential and inhibitory to development of hepatic polarity in WIF-B cells. *Am J Physiol Gastrointest Liver Physiol* 2008; 294:G576-88; PMID:18096610; <http://dx.doi.org/10.1152/ajpgi.00159.2007>.
- Son S, Kojima T, Decaens C, Yamaguchi H, Ito T, Imamura M, et al. Knockdown of tight junction protein claudin-2 prevents bile canaliculi formation in WIF-B9 cells. *Histochem Cell Biol* 2009; 131:411-24; PMID:19084987; <http://dx.doi.org/10.1007/s00418-008-0546-0>.
- Montesano R, Friend DS, Perrelet A, Orci L. In vivo assembly of tight junctions in fetal rat liver. *J Cell Biol* 1975; 67:310-9; PMID:1194351; <http://dx.doi.org/10.1083/jcb.67.2.310>.
- Rahner C, Mitic LL, Anderson JM. Heterogeneity in expression and subcellular localization of claudins 2, 3, 4, and 5 in the rat liver, pancreas, and gut. *Gastroenterology* 2001; 120:411-22; PMID:11159882; <http://dx.doi.org/10.1053/j.gast.2001.21736>.

32. Sakaguchi T, Gu X, Golden HM, Suh E, Rhoads DB, Reinecker HC. Cloning of the human claudin-2 5'-flanking region revealed a TATA-less promoter with conserved binding sites in mouse and human for caudal-related homeodomain proteins and hepatocyte nuclear factor-1alpha. *J Biol Chem* 2002; 277:21361-70; PMID:11934881; <http://dx.doi.org/10.1074/jbc.M110261200>.
33. Liu S, Kuo W, Yang W, Liu W, Gibson GA, Dorko K, et al. The second extracellular loop dictates Occludin-mediated HCV entry. *Virology* 2010; 407:160-70; PMID:20822789; <http://dx.doi.org/10.1016/j.virol.2010.08.009>.
34. Fu D, Wakabayashi Y, Ido Y, Lippincott-Schwartz J, Arias IM. Regulation of bile canalicular network formation and maintenance by AMP-activated protein kinase and LKB1. *J Cell Sci* 2010; 123:3294-302; PMID:20826460; <http://dx.doi.org/10.1242/jcs.068098>.
35. Martinez-Palomo A, Meza I, Beaty G, Cerejido M. Experimental modulation of occluding junctions in a cultured transporting epithelium. *J Cell Biol* 1980; 87:736-45; PMID:6780571; <http://dx.doi.org/10.1083/jcb.87.3.736>.
36. Samarin SN, Ivanov AI, Flatau G, Parkos CA, Nusrat A. Rho/Rho-associated kinase-II signaling mediates disassembly of epithelial apical junctions. *Mol Biol Cell* 2007; 18:3429-39; PMID:17596509; <http://dx.doi.org/10.1091/mbc.E07-04-0315>.
37. Pitelka DR, Taggart BN, Hamamoto ST. Effects of extracellular calcium depletion on membrane topography and occluding junctions of mammary epithelial cells in culture. *J Cell Biol* 1983; 96:613-24; PMID:6403552; <http://dx.doi.org/10.1083/jcb.96.3.613>.
38. Furuse M, Furuse K, Sasaki H, Tsukita S. Conversion of zonulae occludentes from tight to leaky strand type by introducing claudin-2 into Madin-Darby canine kidney 1 cells. *J Cell Biol* 2001; 153:263-72; PMID:11309408; <http://dx.doi.org/10.1083/jcb.153.2.263>.
39. Amasheh S, Meiri N, Gitter AH, Schöneberg T, Mankertz J, Schulzke JD, et al. Claudin-2 expression induces cation-selective channels in tight junctions of epithelial cells. *J Cell Sci* 2002; 115:4969-76; PMID:12432083; <http://dx.doi.org/10.1242/jcs.00165>.
40. McNeill H, Ozawa M, Kemler R, Nelson VJ. Novel function of the cell adhesion molecule uvomorulin as an inducer of cell surface polarity. *Cell* 1990; 62:309-16; PMID:2164888; [http://dx.doi.org/10.1016/0092-8674\(90\)90368-O](http://dx.doi.org/10.1016/0092-8674(90)90368-O).
41. Bazellieres E, Assemat E, Arsanto JP, Le Bivic A, Massey-Harroche D. Crumbs proteins in epithelial morphogenesis. *Front Biosci* 2009; 14:2149-69; PMID:19273190; <http://dx.doi.org/10.2741/3368>.
42. Coleman R, Roma MG. Hepatocyte couples. *Biochem Soc Trans* 2000; 28:136-40; PMID:10816115.
43. Takaki Y, Hirai S, Manabe N, Izumi Y, Hirose T, Nakaya M, et al. Dynamic changes in protein components of the tight junction during liver regeneration. *Cell Tissue Res* 2001; 305:399-409; PMID:11572093; <http://dx.doi.org/10.1007/s004410100397>.
44. Balkovetz DF. Claudins at the gate: determinants of renal epithelial tight junction paracellular permeability. *Am J Physiol Renal Physiol* 2006; 290:F572-9; PMID:16461756; <http://dx.doi.org/10.1152/ajprenal.00135.2005>.
45. Elkouby-Naor L, Ben-Yosef T. Functions of claudin tight junction proteins and their complex interactions in various physiological systems. *Int Rev Cell Mol Biol* 2010; 279:1-32; PMID:20797675; [http://dx.doi.org/10.1016/S1937-6448\(10\)79001-8](http://dx.doi.org/10.1016/S1937-6448(10)79001-8).
46. Mandel LJ, Bacallao R, Zampighi G. Uncoupling of the molecular 'fence' and paracellular 'gate' functions in epithelial tight junctions. *Nature* 1993; 361:552-5; PMID:8429911; <http://dx.doi.org/10.1038/361552a0>.
47. Takakuwa R, Kokai Y, Kojima T, Akatsuka T, Tobioka H, Sawada N, et al. Uncoupling of gate and fence functions of MDCK cells by the actin-depolymerizing reagent mycalolide B. *Exp Cell Res* 2000; 257:238-44; PMID:10837137; <http://dx.doi.org/10.1006/excr.2000.4887>.
48. Gonzales-Mariscal L, Avila A, Betanzos A. The relationship between structure and functions of tight junctions. In Cerejido M, Anderson J, eds. *Tight junctions*. Second edition. Boca Raton. CRC Press 2001:89-120.
49. Bender V, Bravo P, Decaens C, Cassio D. The structural and functional polarity of the hepatic human/rat hybrid WIF-B is a stable and dominant trait. *Hepatology* 1999; 30:1002-10; PMID:10498653; <http://dx.doi.org/10.1002/hep.510300436>.
50. Stammerl L, Reichen J, Oehler R, Bianchi L, Landmann L. Decreased hepatocellular volume and intact morphology of tight junctions in calcium deprivation-induced cholestasis. Stereological and multiple indicator dilution analysis. *J Hepatol* 1990; 10:318-26; PMID:2195107; [http://dx.doi.org/10.1016/0168-8278\(90\)90139-1](http://dx.doi.org/10.1016/0168-8278(90)90139-1).
51. Cohen D, Tian Y, Müsch A. Par1b promotes hepatic-type lumen polarity in Madin Darby canine kidney cells via myosin II- and E-cadherin-dependent signaling. *Mol Biol Cell* 2007; 18:2203-15; PMID:17409351; <http://dx.doi.org/10.1091/mbc.E07-02-0095>.
52. Tsukada N, Ackerley CA, Phillips MJ. The structure and organization of the bile canalicular cytoskeleton with special reference to actin and actin-binding proteins. *Hepatology* 1995; 21:1106-13; PMID:7705786.
53. Ivanov AI. Actin motors that drive formation and disassembly of epithelial apical junctions. *Front Biosci* 2008; 13:6662-81; PMID:18508686; <http://dx.doi.org/10.2741/3180>.
54. Van Itallie C, Rahner C, Anderson JM. Regulated expression of claudin-4 decreases paracellular conductance through a selective decrease in sodium permeability. *J Clin Invest* 2001; 107:1319-27; PMID:11375422; <http://dx.doi.org/10.1172/JCI12464>.
55. Yu AS, Enck AH, Lencer WI, Schneeberger EE. Claudin-8 expression in Madin-Darby canine kidney cells augments the paracellular barrier to cation permeation. *J Biol Chem* 2003; 278:17350-9; PMID:12615928; <http://dx.doi.org/10.1074/jbc.M213286200>.
56. Amasheh S, Schmidt T, Mahn M, Florian P, Mankertz J, Tavalali S, et al. Contribution of claudin-5 to barrier properties in tight junctions of epithelial cells. *Cell Tissue Res* 2005; 321:89-96; PMID:16158492; <http://dx.doi.org/10.1007/s00441-005-1101-0>.
57. Michikawa H, Fujita-Yoshigaki J, Sugiya H. Enhancement of barrier function by overexpression of claudin-4 in tight junctions of submandibular gland cells. *Cell Tissue Res* 2008; 334:255-64; PMID:18855016; <http://dx.doi.org/10.1007/s00441-008-0689-2>.
58. Hoewel T, Macek R, Mundigl O, Swisshelm K, Kubbies M. Expression and targeting of the tight junction protein CLDN1 in CLDN1-negative human breast tumor cells. *J Cell Physiol* 2002; 191:60-8; PMID:11920682; <http://dx.doi.org/10.1002/jcp.10076>.
59. Rossa J, Lorenz D, Ringling M, Veshnyakova A, Piontek J. Overexpression of claudin-5 but not claudin-3 induces formation of trans-interaction-dependent multilamellar bodies. *Ann N Y Acad Sci* 2012; 1257:59-66; PMID:22671590; <http://dx.doi.org/10.1111/j.1749-6632.2012.06546.x>.
60. Furuse M. Knockout animals and natural mutations as experimental and diagnostic tool for studying tight junction functions in vivo. *Biochim Biophys Acta* 2009; 1788:813-9; PMID:18706387; <http://dx.doi.org/10.1016/j.bbame.2008.07.017>.
61. Hou J, Gomes AS, Paul DL, Goodenough DA. Study of claudin function by RNA interference. *J Biol Chem* 2006; 281:36117-23; PMID:17018523; <http://dx.doi.org/10.1074/jbc.M608853200>.
62. McNeil E, Capaldo CT, Macara IG. Zonula occludens-1 function in the assembly of tight junctions in Madin-Darby canine kidney epithelial cells. *Mol Biol Cell* 2006; 17:1922-32; PMID:16436508; <http://dx.doi.org/10.1091/mbc.E05-07-0650>.
63. Hernandez S, Chavez Munguia B, Gonzalez-Mariscal L. ZO-2 silencing in epithelial cells perturbs the gate and fence function of tight junctions and leads to an atypical monolayer architecture. *Exp Cell Res* 2007; 313:1533-47; PMID:17374535; <http://dx.doi.org/10.1016/j.yexcr.2007.01.026>.
64. Capaldo CT, Macara IG. Depletion of E-cadherin disrupts establishment but not maintenance of cell junctions in Madin-Darby canine kidney epithelial cells. *Mol Biol Cell* 2007; 18:189-200; PMID:17093058; <http://dx.doi.org/10.1091/mbc.E06-05-0471>.
65. Cohen D, Brennwald PJ, Rodriguez-Boulan E, Müsch A. Mammalian PAR-1 determines epithelial lumen polarity by organizing the microtubule cytoskeleton. *J Cell Biol* 2004; 164:717-27; PMID:14981097; <http://dx.doi.org/10.1083/jcb.200308104>.
66. Cohen D, Rodriguez-Boulan E, Müsch A. Par-1 promotes a hepatic mode of apical protein trafficking in MDCK cells. *Proc Natl Acad Sci U S A* 2004; 101:13792-7; PMID:15365179; <http://dx.doi.org/10.1073/pnas.0403684101>.
67. Eisen R, Walid S, Ratcliffe DR, Ojakian GK. Regulation of epithelial tubule formation by Rho family GTPases. *Am J Physiol Cell Physiol* 2006; 290:C1297-309; PMID:16338972; <http://dx.doi.org/10.1152/ajpcell.00287.2005>.
68. Chaumontet C, Mazzoleni G, Decaens C, Bex V, Cassio D, Martel P. The polarized hepatic human/rat hybrid WIF 12-1 and WIF-B cells communicate efficiently in vitro via connexin 32-constituted gap junctions. *Hepatology* 1998; 28:164-72; PMID:9657109; <http://dx.doi.org/10.1002/hep.510280122>.
69. Kojima T, Sawada N, Yamaguchi H, Fort AG, Spray DC. Gap and tight junctions in liver: composition, regulation and function. In Arias IM ed. *The liver biology and pathobiology*. Fifth edition. Wiley-Blackwell publication. 2009:201-220.
70. Vinken M, Papeleu P, Snykers S, De Rop E, Henkens T, Chipman JK, et al. Involvement of cell junctions in hepatocyte culture functionality. *Crit Rev Toxicol* 2006; 36:299-318; PMID:16809101; <http://dx.doi.org/10.1080/10408440600599273>.
71. Fu D, Wakabayashi Y, Lippincott-Schwartz J, Arias IM. Bile acid stimulates hepatocyte polarization through a cAMP-Epac-MEK-LKB1-AMPK pathway. *Proc Natl Acad Sci U S A* 2011; 108:1403-8; PMID:21220320; <http://dx.doi.org/10.1073/pnas.1018376108>.
72. Zegers MM, O'Brien LE, Yu W, Datta A, Mostov KE. Epithelial polarity and tubulogenesis in vitro. *Trends Cell Biol* 2003; 13:169-76; PMID:12667754; [http://dx.doi.org/10.1016/S0962-8924\(03\)00036-9](http://dx.doi.org/10.1016/S0962-8924(03)00036-9).
73. Martín-Belmonte F, Yu W, Rodríguez-Fraticelli AE, Ewald AJ, Werb Z, Alonso MA, et al. Cell-polarity dynamics controls the mechanism of lumen formation in epithelial morphogenesis. [Erratum in: *Curr Biol* 2008; 18:1016. *Curr Biol* 2008; 18:630. Ewald, Andrew] [corrected to Ewald, Andrew J]. *Curr Biol* 2008; 18:507-13; PMID:18394894; <http://dx.doi.org/10.1016/j.cub.2008.02.076>.
74. Naydenov NG, Ivanov AI. Spectrin-adducin membrane skeleton: A missing link between epithelial junctions and the actin cytoskeleton? *BioArchitecture* 2011; 4:186-91; <http://dx.doi.org/10.4161/bioa.1.4.17642>.
75. Cardellini P, Davanzo G, Citi S. Tight junctions in early amphibian development: detection of junctional cingulin from the 2-cell stage and its localization at the boundary of distinct membrane domains in dividing blastomeres in low calcium. *Dev Dyn* 1996; 207:104-13; PMID:8875080; [http://dx.doi.org/10.1002/\(SICI\)1097-0177\(199609\)207:1<104::AID-AJA10>3.0.CO;2-0](http://dx.doi.org/10.1002/(SICI)1097-0177(199609)207:1<104::AID-AJA10>3.0.CO;2-0).

-
76. Stevenson BR, Siliciano JD, Mooseker MS, Goodenough DA. Identification of ZO-1: a high molecular weight polypeptide associated with the tight junction (zonula occludens) in a variety of epithelia. *J Cell Biol* 1986; 103:755-66; PMID:3528172; <http://dx.doi.org/10.1083/jcb.103.3.755>.
77. Combettes L, Tran D, Tordjmann T, Laurent M, Berthon B, Claret M. Ca(2+)-mobilizing hormones induce sequentially ordered Ca2+ signals in multicellular systems of rat hepatocytes. *Biochem J* 1994; 304:585-94; PMID:7998996.
78. Simionescu N, Simionescu M. Galloylglucoses of low molecular weight as mordant in electron microscopy. I. Procedure, and evidence for mordanting effect. *J Cell Biol* 1976; 70:608-21; PMID:783172; <http://dx.doi.org/10.1083/jcb.70.3.608>.
79. Bender V, Büschlen S, Cassio D. Expression and localization of hepatocyte domain-specific plasma membrane proteins in hepatoma x fibroblast hybrids and in hepatoma dedifferentiated variants. *J Cell Sci* 1998; 111:3437-50; PMID:9788884.
80. Pagano RE, Martin OC. A series of fluorescent N-acylsphingosines: synthesis, physical properties, and studies in cultured cells. *Biochemistry* 1988; 27:4439-45; PMID:3166987; <http://dx.doi.org/10.1021/bi00412a034>.